NRC Publications Archive
Archives des publications du CNRC

Towards improving the practical energy density of Li-ion batteries: optimization and evaluation of silicon: graphite composites in full cells
Yim, Chae-Ho; Niketic, Svetlana; Salem, Nuha; Naboka, Olga; Abu-lebdeh, Yaser

National Research Council Canada   Conseil national de recherches Canada

Canada

Towards Improving the Practical Energy Density of Li-Ion Batteries: Optimization and Evaluation of Silicon:Graphite Composites in Full Cells

Chae-Ho Yim, Svetlana Niketic, Nuha Salem, Olga Naboka, and Yaser Abu-Lebdeh[z]

Energy, Mining and Environment Portfolio and Automotive and Surface Transportation Portfolio, National Research Council of Canada, Ottawa, Ontario K1A 0R6, Canada

Increasing the energy density of Li-ion batteries is very crucial for the success of electric vehicles, grid-scale energy storage, and next-generation consumer electronics. One popular approach is to incrementally increase the capacity of the graphite anode by integrating silicon into composites with capacities between 500 and 1000 mAh/g as a transient and practical alternative to the more-challenging, silicon-only anodes. In this work, we have calculated the percentage of improvement in the capacity of silicon:graphite composites and their impact on energy density of Li-ion full cell. We have used the Design of Experiment method to optimize composites using data from half cells, and it is found that 16% improvements in practical energy density of Li-ion full cells can be achieved using 15 to 25 wt% of silicon. However, full-cell assembly and testing of these composites using $LiNi_{0.5}Mn_{0.5}Co_{0.5}O_2$ cathode have proven to be challenging and composites with no more than 10 wt% silicon were tested giving 63% capacity retention of 95 mAh/g at only 50 cycles. The work demonstrates that introducing even the smallest amount of silicon into graphite anodes is still a challenge and to overcome that improvements to the different components of the Li-ion battery are required.

Most commercial Li-ion batteries still use carbon as an anode material since they were first commercialized in 1991 due to its low cost and excellent electrochemical performance especially long battery cycle life.[1] However, the reversible electrochemical intercalation of Li^+ into the graphite structure is limited to one lithium per six carbons (LiC_6) that results in a theoretical capacity of 372 mAh/g. To that end, there are on-going efforts to explore higher capacity anode materials, to meet the increasing demand for batteries with higher energy density. This is done by exploring materials that are based on storing and releasing Li^+ ion by electrochemical mechanisms other than intercalation such as electrochemical alloying e.g. tin,[2] and silicon[3] or their composites(Sn-Co-C),[4,5] or conversion reaction, mostly in oxides[6] of transition metals such as Co, Ni, Cu or Fe, or mixed oxides such as spinel-like $ZnMn_2O_4$.[7] However, the battery performance of both types is still not promising as they show: poor electronic conductivity, high irreversible first-cycle capacity, high insertion/conversion potential, large volume expansion and large hysteresis in potential during cycling.

The most promising materials that are currently under extensive R&D and have better chance to replace carbon are elements (mostly metals) that can electrochemically alloy with lithium (Si, Al, Sn, Ge, Bi, Sb, Ag, Mg, Pb). Table I shows the theoretical capacity of elements that can alloy with lithium. It is clear that silicon has the highest capacity reaching 4200 mAh/g (gravimetric) and 9800 mAh/cm^3(volumetric). Germanium has the second highest gravimetric and volumetric capacity. This is due to the higher density of germanium as shown in Table I. Aluminum has a similar density to silicon, however, due to the lower molar interaction with lithium (limited to 1:1) gave much lower capacity than other metals. Even though aluminum has low specific capacity among the metals, it has the highest electrical conductivity that can reduce polarization resistance during charge/discharge and hence improve the battery performance.

Silicon is very attractive since it comes from an abundant source; it is cheap and has a high theoretical capacity of 4200 mAh/g.[8,9] It reacts with lithium by forming the alloy $SiLi_x$ with $0 \leq x \leq 4.4$. Taking such a high quantity of lithium involves large structural (volume) changes that can reach up to 400%.[1,10,11] This gives rise to mechanical stresses that lead to pulverization of silicon structure associated with solid electrolyte interface (SEI) formation that eventually cause the failure of the battery.[12] Many solutions to the problem have been proposed: (1) The use of nano-sized or nanostructured silicon that usually provides higher experimental capacity and better capacity retention[8,13–15] because the volume change can be accommodated by free volume or fast stress relaxation. (2) The use of silicon/metal composite where the metal that does not alloy with Li^+ acts as a matrix that minimizes the volume expansion.[7,16,17] (3) The use of an upper limit on the capacity to make silicon alloy only partially with Li^+ to control volume changes.[18] (4) The use of new binders that can accommodate the volume expansion better than the conventional binder: polyvinylidene fluoride (PVDF).[19–22] Examples of the binders investigated in this regard are: alginic acid (AA),[23] polyamide-imide (PAI),[24] sodium or lithium salts of polyacrylic acid (NaPAA or LiPAA),[14,22,25] polyimide (PI),[26] sodium or lithium salts of carboxymethyl cellulose (NaCMC or LiCMC).[21] and conductive binders[27,28] (5) The use of silicon in a composite at low content typically and preferably less than 20 wt% with graphitic carbon because of its great physical and chemical properties. This leads to lower anode capacity values than using Si alone, but it shows better capacity retention with good cycle life. This solution gained a lot of popularity among researchers and manufacturers as a short-term alternative to graphite because of the experimental difficulties faced in achieving total silicon capacity with enough cycle life. Graphitic carbon in itself is still interesting as an anode material and chances are it will be used in commercial batteries as the main anode material for some time due to mature manufacturing processes and good battery performance. In this regard, it is considered as a diluent/buffer to mitigate the total volume expansion of the composite by using less of the metals that can also lower the cost when the element is more expensive than carbon.

In this paper, we have studied silicon along with other elements that can alloy with lithium to optimize the capacity of their composite with graphitic carbon and evaluate their impact on the practical energy density of full Li-ion cell. We have modified a cell-based model developed by Obravac et al.[29] and applied it to silicon/graphitic carbon composites and we have observed improvements in the energy density of the Li-ion full cell using different cathode materials. The design of the experiment method has been used to optimize the capacity of

[z]E-mail: Yaser.Abu-Lebdeh@nrc-cnrc.gc.ca

Table I. Specification of Li alloyable metals.

Elements	Si	Sn	Al	Ge	Bi	Sb
Density (g/cm^3)	2.3	5.8	2.7	5.3	9.8	6.7
Conductivity (S/m)	1×10^3	9.1×10^6	3.8×10^7	2×10^3	7.7×10^5	2.5×10^6
Gravimetric Capacity (mAh/g)	4200	959	993	1600	385	660
Volumetric Capacity (mAh/cm^3)	9782	7063	2681	8526	3765	4422
Average potential (V)	0.40	0.50	0.38	0.60	3.3	0.95

the composite by identifying the variables that significantly affects its performance in the battery.

Experimental

Materials.—Silicon (nanopowder, ∼100 nm), ethylene carbonate (EC, anhydrous, 99%), dimethyl carbonate (DMC, anhydrous, 99%) and N-methyl-pyrrolinone (NMP, anhydrous, 99.5%) were obtained from Sigma-Aldrich. Carbon graphite KS-4 and Super S carbon were obtained from Lonza G+T (Switzerland) and Timcal (Switzerland), respectively. Sodium carboxymethyl cellulose (NaCMC, viscosity 42.0 mPa s) was purchased from Calbiochem. LiMn$_{1/3}$Ni$_{1/3}$Co$_{1/3}$O$_2$ (NMC) was obtained from 3 M.

Synthesis of etched nano silicon.—Si nanopowder was dispersed in 1 M HF and sonicated for 20 min and then washed with ethanol using a centrifuge. The washed sample was dried in vacuum oven at 80°C overnight. The dried sample was used for further characterization and analysis.

Characterization.—Battery cycling was carried out on half and full-cells using 2325-type coin cells (supplied by National Research Council of Canada) assembled in an argon-filled dry glove box. Capacity measurements were performed by galvanostatic experiments carried out on a multichannel Arbin battery cycler (BT2000). The working electrode was first discharged (lithiated) down to 5 mV and then charged (delithiated) up to 1.5 V versus Li/Li+ galvanostatically for half-cells. The electrode anode and cathode films were prepared on a high purity copper and an aluminum foil current collector, respectively, (copper foil was cleaned using a 2.5% HCl solution in order to remove the copper oxide layer) using an automated doctor-blade and then dried overnight at 85°C in a convection oven. Individual disk electrodes (Ø = 12.5 mm) were punched out, dried at 80°C under vacuum overnight and then pressed under a pressure of 0.5 metric ton. Electrodes were made of 3–4 mg of the active material. A lithium metal disk (Ø = 16.5 mm) was used as a negative electrode (counter electrode and reference electrode). 70 µL of an electrolyte solution of 1 M LiPF$_6$ in ethylene carbonate–dimethyl carbonate (EC:DMC, 1:1, v/v) or ethylene carbonate-diethyl carbonate (EC:DEC, 3:7, v:v) with 10% fluoroethylene carbonate (FEC) was spread over a double layer of microporous polypropylene separators (Celgard 3501 for EC:DMC or Celgard 2500 for EC:DEC, thickness = 30 µm, Ø = 21 mm). The cells were assembled in an argon-filled dry glove box at room temperature and rested overnight before testing.

Results and Discussion

Comparison of theoretical capacity of alloyable elements and their composites.—*Calculations of effect of anode and cathode specific (gravimetric) capacity on the energy density of full-cells based on active materials only.*—Increasing the specific capacity of the anode can lead to improvement of total cell capacity, however, as others and we have discussed previously,[11,30] high capacity of the anode materials is not necessary unless the cathode capacity also improves. To evaluate the effect of the anode specific discharge capacity of the full-cell capacity, we have followed the approach introduced by Kasavajjula et al.[11] who used Equation 1 to calculate the total cell capacity using commercial 18560 cylindrical cell assuming cathode capacity of
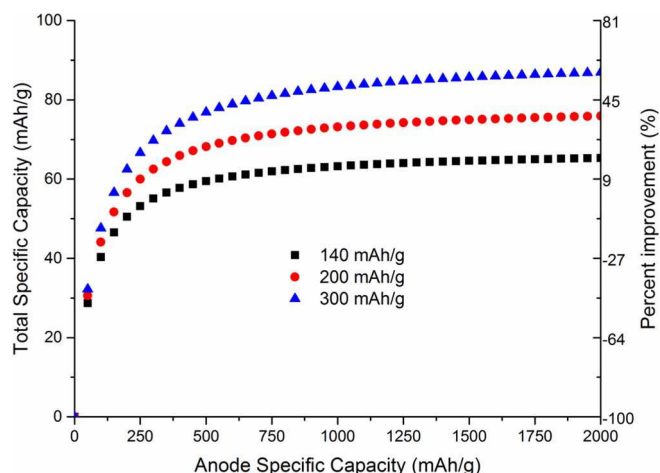
140 and 200 mAh/g. They reviewed methodologies to prevent the capacity fade of silicon-based anode material. We have reproduced the results for the cathodes with 140 and 200 mAh/g capacity as shown in Figure 1, but also extended the calculations to cathodes with higher capacity (300 mAh/g) and also calculated the percentage of improvement in total cell capacity compared to commonly used materials graphite and LiCoO$_2$. Figure 1 shows the total cell capacity of a commercial 18560 cylindrical cells as a function of the anode specific capacity calculated using Equation 1. The figure clearly shows that in all cases a noticeable rapid increase of the total cell capacity occurs up until the anode capacity reaches 1000 mAh/g. Above this value, the improvement in capacity is marginal and can be considered of low value when cost and other factors are taking into account.

$$\text{Total cell } (mAh/g) = \frac{1}{(1/Q_A) + (1/Q_C) + (1/Q_M)} \qquad [1]$$

Q_A and Q_C: anode and cathode specific capacity (mAh/g)
Q_M: Mass of inactive materials (mAh/g)

Figure 1 also shows (the secondary y-axis) the percentage of improvement in the total cell capacity in a commercial battery as a base where anode and cathode capacities are 300 and 140 mAh/g, respectively. Keeping anode capacity at 300 mAh/g and increasing the cathode capacity results in an increase in the total capacities by 13 and 27% for 200 and 300 mAh/g of cathode capacities, respectively. However, when the anode capacities are at 1000 mAh/g the total capacities increase by 33 and 51% for 200 and 300 mAh/g cathode capacities, respectively. Also, an increase of 15% in the total capacity can still be achieved with 140 mAh/g of cathode capacity.

The calculations above are only a rough approximation and very useful in demonstrating the effect of changes to the capacity of either the anode or the cathode materials on the total capacity. In commercial batteries, other factors have to be taking into accounts such as volume, voltages, irreversible capacities, electrode formulations, processing and geometrical factors.

Figure 1. Target capacity and improvement in energy density to the current Li-ion battery calculated using Equation 1.

Figure 2. Gravimetric and volumetric energy density of alloyable elements vs volume expansion.

Calculations of the energy density of alloyable elements.—In commercial batteries, the energy density is one of the most important features as it takes into account not only capacity but also voltage, weight, and volume of all active and inactive components. The volumetric energy density is calculated using the average difference in potential between cathode and anode and the molar volume as shown in Equation 2. The average potentials for anodes are listed in Table I. The volumetric energy density is plotted as a function of volume expansion calculated using Equation 2 and Equation 3,[31] where Equation 3 is the volume expansion as a function of a number of moles of lithium per mole of host alloy atoms. The results are plotted in Figure 2. Plotting energy density vs volume expansion rather than the number of moles is more useful as it provides a better guide, later on, to choose the alloyable element at a certain energy density and a tolerable volume expansion. For all the elements, the capacity increases as a simple rational function. It is clear that silicon has the highest energy density but also the highest volume expansion. The difference in the volumetric energy density of all the elements is not significant due to the very high density of the metals of lowest capacities (Sn, Ge, Sb) which also offsets the high average voltage. However, their gravimetric energy density varies significantly while silicon still giving the highest values followed by aluminum while the other three gave much lower values, as shown in Figure 2.

$$\tilde{U} = \frac{-\int_{x=x_f}^{0} \left[V_{(+)}(x) - V_{(-)}(x) \right] F dx}{v(x_f)} \quad [2]$$

$$\xi = \frac{kx}{v_0} \times 100\% \quad [3]$$

$\tilde{U}$: Volumetric energy density
x: Number of moles of lithium per mole of host alloy atoms

x_f: Number of moles of lithium per mole of host alloy atoms at full lithiation
$V_{(+)}$ or $V_{(-)}$: Cathode and anode voltage
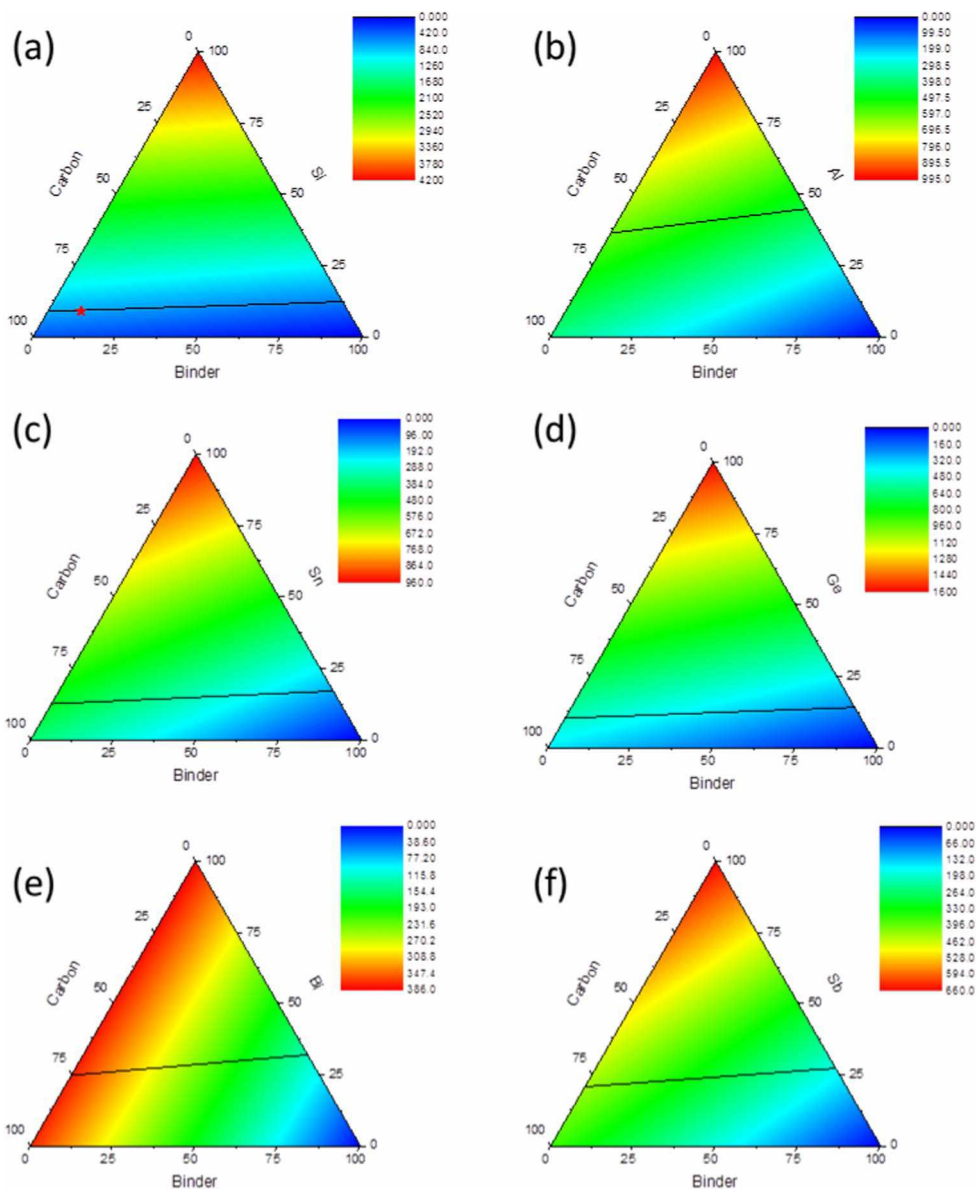F: Faraday's number, 26.802 Ah/mol
v: Molar volume of the alloy anode
k: Molar volume of lithium in metal alloy
v_0: Unlithiated molar volume of the alloy

Calculation of the capacity of composites (alloyable element: graphitic carbon).—The theoretical capacity of composites made of two electrochemically active components: alloyable element (Si, Al, Sn, Ge, Sb, Bi) and graphitic carbon, and inactive component: polymeric binder were calculated and are shown as ternary diagrams in Figure 3. The capacities were calculated by multiplying the percentage of each of the active components by its theoretical capacity and divided by the total (active and inactive) weight. 375 mAh/g of graphite capacity was used while the values for the alloyable elements were taken from Table I. The volume expansion of the composite was calculated assuming that volume changes for the binder and graphitic carbon are 0 and 12%,[32] respectively, while the volume expansions of the alloyable elements are the maximum expansion at the fully lithiated state obtained from Equation 3. The color in the ternary diagram highlights the variation in the theoretical capacity of the composite as a function of the three components in the fully lithiated state. We have also outlined the composites at volume expansion of 40%. This value was chosen in order to simulate the available free "void" within a commercial battery composite that can accommodate the increase in volume when it is lithiated from the delithiated state.[33–36] For all the alloyable elements, the capacity of the composite was highest when the element content was maximum (red region of the diagrams) except for Bi because of its lower capacity compared to graphite. Again, silicon gives the highest capacity values in composites compared to the other elements. The black line, which represents the 40% capacity expansion, crosses composites with a large variation in capacity and Table II shows the minimum and maximum capacity for these composites.

At 40% volume expansion, the maximum capacity achieved for a composite is 715 mAh/g with 9 wt% silicon and 91 wt% graphite), when no binder is used that is also a point where the carbon axis and the black line meet in the ternary diagram in Figure 3. The minimum capacity of 518 mAh/g is obtained in a composite of 12% silicon and 88% binder, which is at the opposite side of the black line of the maximum capacity. In between, there is a whole range of compositions that can be selected based on the application. In commercial batteries, around 10% of binder and carbon additive is used and we will assume the amount of binder represent the total of the two, i.e. carbon additive has a negligible contribution to capacity. Also shown in Table II are the capacities for the practical composite (composites with 10% binder) calculated for all the elements. In the case of Si, this practical composite is composed of 10% binder, 9% Si, and 81% graphite and shows 692 mAh/g of reversible capacity, highlighted as a red star in the diagram. The results from Figure 3 and Table II clearly show that silicon is the best element to use on its own, if possible, or in a composite to achieve the highest capacity in a battery, despite its high volume expansion which as we have shown can be controlled to certain tolerable values such as the 40% volume expansion. If more capacity is needed, higher volume expansions will take place, and therefore Table III shows calculated volume expansion for composites with Si and Ge for capacity limited to 1000 and 1300 mAh/g. It shows that to get a higher practical capacity reaching 1000 mAh/g double the amount of silicon (17%) is needed, but with much higher volume expansion (65%) compared to the composite with 40% volume expansion.

As the elements have different volume expansions, capacities, and voltages, it is tempting to see the effect of incorporating more than one of the elements into a composite to get higher capacities and lower volume expansion. To study the effect of two mixtures of elements, silicon and aluminum were chosen and a ternary diagram is generated and included in supporting information. The maximum capacity at 40% is 517 mAh/g that is lower than the silicon and graphite mix.

Figure 3. Theoretical capacity of the alloyable element: graphitic carbon: polymeric binder composite for (a) silicon, (b) aluminum, (c) tin, (d) germanium, (e) bismuth, and (f) antimony.

Table II. Capacity of the electrode composite with the ratio at 40% volume expansion.

Metals	Capacity (mAh/g)			Ratio (Element: Graphite: Binder)		
	Min	Practical	Max	Min	Practical	Max
Si	518	692	715	0.12: 0: 0.88	0.09:0.81:0.10	0.09: 0.91: 0
Al	446	570	598	0.45: 0: 0.55	0.38:0.52:0.10	0.36: 0.64: 0
Sn	164	412	446	0.17: 0: 0.83	0.13:0.77:0.10	0.13: 0.87: 0
Ge	226	467	499	0.14: 0: 0.86	0.11:0.79:0.10	0.10: 0.90: 0
Bi	123	338	375	0.32: 0: 0.68	0.26:0.64:0.10	0.25: 0.75: 0
Sb	179	397	432	0.27: 0: 0.73	0.22:0.68:0.10	0.21: 0.79: 0

Table III. Volume expansion and electrode composite at 1000 mAh/g and 1300 mAh/g (to include Irr.Cap.).

Metals	Volume expansion (%)			Ratio (Element: Graphite: Binder)		
	Min	Practical	Max	Min	Practical	Max
Si	63	65	77	0.29:0.71:0.00	0.17:0.73:0.10	0.24:0.00:0.76
Ge	151	158	177	0.51:0.49:0.00	0.54:0.36:0.10	0.63:0.00:0.38

Table IV. Properties used in Equation 4 to generate Figure 4.

		Density (mg/L)	$V_{average}$ (V)	Reversible capacity (mAh/g)	Irreversible capacity (%)	Active volume (%)
Cathode	LCO	5.05	3.9	150	6	70
	NMC	4.77	3.7	163	6	70
	LMNO	4.45	4.7	147	6	70
Anode	Graphite	2.26	0.125	350	6	70
	Si	2.3	0.4	3579	6	70

The cause of the low capacity with the two elements is due to the volume expansion. In comparison, from silicon and graphite mix, the graphite has insignificant expansion compared to the metals that help to minimize the volume expansion and improve the capacity. The 40% volume expansion line lies on the right side of the triangle that suggests the use of more than 55% binder, which is not practical. Ternary capacity diagram of Si, Al, and carbon with 10% binder is also provided in supporting information. A table is also provided to show the capacity and the ratio of the mixtures. The maximum capacity was achieved when no aluminum is mixed. This is because even though aluminum provides three times more capacity than graphite; it increases the volume expansion by eight times, which makes this approach not practical.

Energy density improvements of full cells with silicon-based anode.—It is apparent from calculations that so far silicon is the best alloying element to improve the capacity of the anode. However, there is still a need to see whether this will lead to an improvement in the total cell capacity. Obrovac et al.[29] have recently discussed the key parameters that affect the total capacity of the battery. We have used their equation (equation 15 in Obrovac et al.[29]) as a starting point to calculate the energy density of the full cells and modified it by introducing initial columbic efficiency (φ_0^+ and φ_0^-) and volumes of inactive components and other volumes such as porosity of active component.

$$\check{U}_R = \frac{2\tilde{q}_R^+ t^+}{t_{cc}^+ + t_{cc}^- + 2t_s + 2t^+ \left[1 + \frac{\tilde{q}_R^+ \varphi_0^-}{\tilde{q}_R^- \varphi_0^+}\left(\frac{N}{P}\right)\right]}\left(V_{avg}^+ - V_{avg}^-\right) \qquad [4]$$

t^+: Thickness of cathode
t_{cc}^+ and t_{cc}^-: Thickness of anode and cathode current collector
t_s: Thickness of separator
$\tilde{q}_R^+$ and $\tilde{q}_R^-$: Reversible capacity of anode and cathode
φ_0^+ and φ_0^-: Initial columbic efficiency of anode and cathode

N/P: Negative to positive capacity ratio
V_{avg}^+ and V_{avg}^-: Average voltage of anode and cathode

Firstly, the energy density was calculated when silicon only, not a composite, was used as an anode with different cathodes as a function of the first-cycle irreversible capacity of the silicon. The thickness of the cathode and anode current collectors was 15 um. The thickness of the separator was 20 um. The negative/positive (N/P) ratio was 1.1. Other parameters are summarized in Table IV. Figure 4 shows the percentage of improvement in full-cell energy density as a function of irreversible capacity. The figure clearly shows that the highest irreversible capacity (intersection with x-axis) that allows for any improvements to the full cells are 33, 31, and 36% for $LiCoO_2$ (LCO), $LiNi_{0.33}Mn_{0.33}Co_{0.33}O_2$ (NMC), and $LiMn_{0.67}Ni_{0.33}O_2$ (LMNO), respectively. It also shows that the maximum improvements are 48, 43, and 58% for LCO, NMC, and LMNO, respectively; when up to 6% of the irreversible capacity of silicon is allowed. This is way less than what is obtained experimentally with silicon in half-cells that usually gives 20%[37] irreversible capacity and corresponds to 15 to 30% overall improvements. However, these improvements are also overestimated since most of the experimental results have shown much lower reversible capacity for silicon-only anode materials.

Secondly, the same equation was used to find the minimum amount of silicon, in a composite, required to improve the performance of the full-cell. Figure 5 shows the improvements as a function of the active volume of silicon. The minimum volume required to achieve the improvements are 8.19, 9.24, and 6.05% for LCO, NMC, and LMNO respectively. These were calculated using the same parameters in Table IV by changing the active volume of silicon. The minimum required silicon is where the theoretical capacity is equivalent to when graphite is used in a full Li-ion battery. This figure looks similar to Figure 1 since the active amount of silicon corresponds to an increase in the anode material. As a result, Figure 5 also shows the larger amount of silicon in a composite, silicon-rich composite, do not give high improvements, instead, volume expansion due to the high amount of silicon will have detrimental effects on the battery performance. This
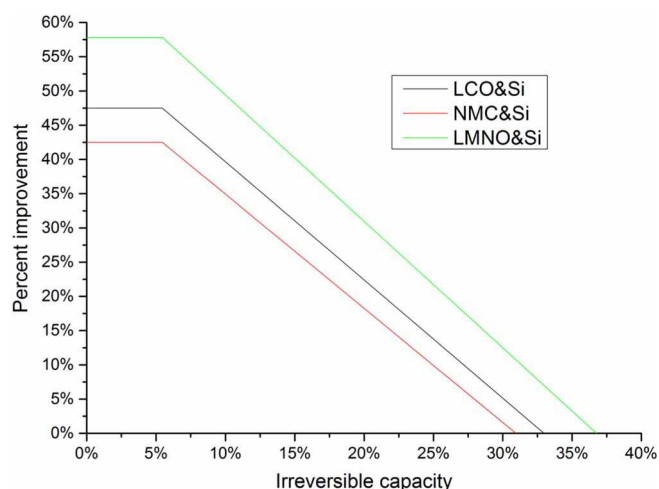

Figure 4. Improvements of the energy density of full-cell when silicon is used as anode with different cathode.
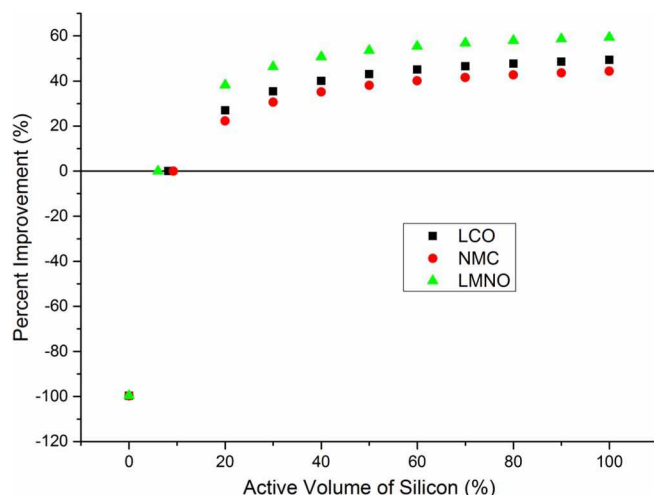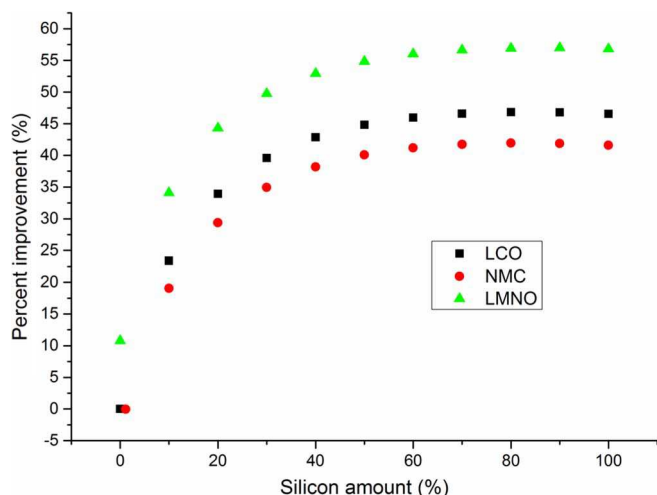

Figure 5. Improvements in energy density as a function of active volume of silicon.
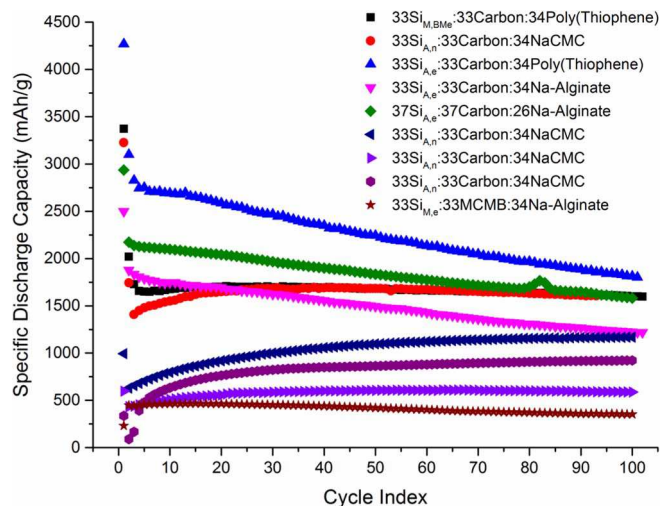
Figure 6. Improvements in energy density of silicon:graphite composite with graphite as a function of silicon contents.

Figure 7. Cycling performance of Li-ion half-cell battery results from various silicon:graphite:binder composites. $Si_{x,y}$ refers to nanosilicon where x refers to the name of the supplier (A for Aldrich, M for MTI), and y refers to the state of silicon (BM for ball-milled, e for etched, n for as-received and non-etched), numbers refer to the amount in percentage of each material in the electrodes.

estimation also assumes fixed and low amount of irreversible capacity of silicon.

Finally, the amount of silicon in a composite was applied into Equation 4 to estimate the improvement and results are shown in Figure 6, which shows the improvements versus silicon/graphite composites. LMNO gave the highest improvement (11%) without even using any silicon due to the high average voltage and capacity. For NMC, 1.1% of silicon has to be used to achieve the minimum improvements. The maximum improvements were achieved around 80 and 90 wt% of silicon composites, silicon-rich composites. 47, 42, and 57% of improvements were achieved for LCO, NMC, and LMNO, respectively. The improvement slows down as the composite becomes very rich in silicon up until 80 wt% of silicon where after less improvement is achieved due to the higher average potential of the silicon that reduces overall potential in a full-cell and consequently reduces the energy density of the full cells.

During the course of this work, Dash et al.[38] used simple mass balance calculations to obtain volumetric capacity and introduced an equation using porosity/volume accommodation parameter to determine the theoretical limits of Si in a Si–carbon composite based anode to maximize the volumetric energy density of Li-ion cells. From calculations, they reported that the level of improvement in volumetric and gravimetric energy density of Li-ion cells using silicon-carbon composite with constrained volume is less than 15% when compared to Li-ion cell using a graphite-only anode.[38]

Performance of silicon/graphite composites in half Li-ion cells.—To verify the calculation, we have assembled and tested coin-type, half and full-cells using Si-carbon composites as an anode, NMC and LMNO as a cathode and a carbonate-based electrolyte. We have

optimized the cell performance by looking into the following parameters: type and amount of electrode components (silicon, graphitic carbon, and binder), type of electrolyte, and "laminate" thickness on the cast, as summarized in Table V. We have used a design of experiment approach to analyzing the data to find optimum performance. Figure 7 shows some of the cycling performance of Li-ion half cells, which are selected to represent various parameters we have tested. It can be seen that:

1. A large irreversible capacity ranging from 15 to 200% corresponding to initial columbic efficiency of 30 to 75%.
2. A reversible capacity ranging from 350 to 2500 mAh/g with the 33 wt% Si-composite giving the highest capacity while composite 11 wt% giving the lowest capacity.
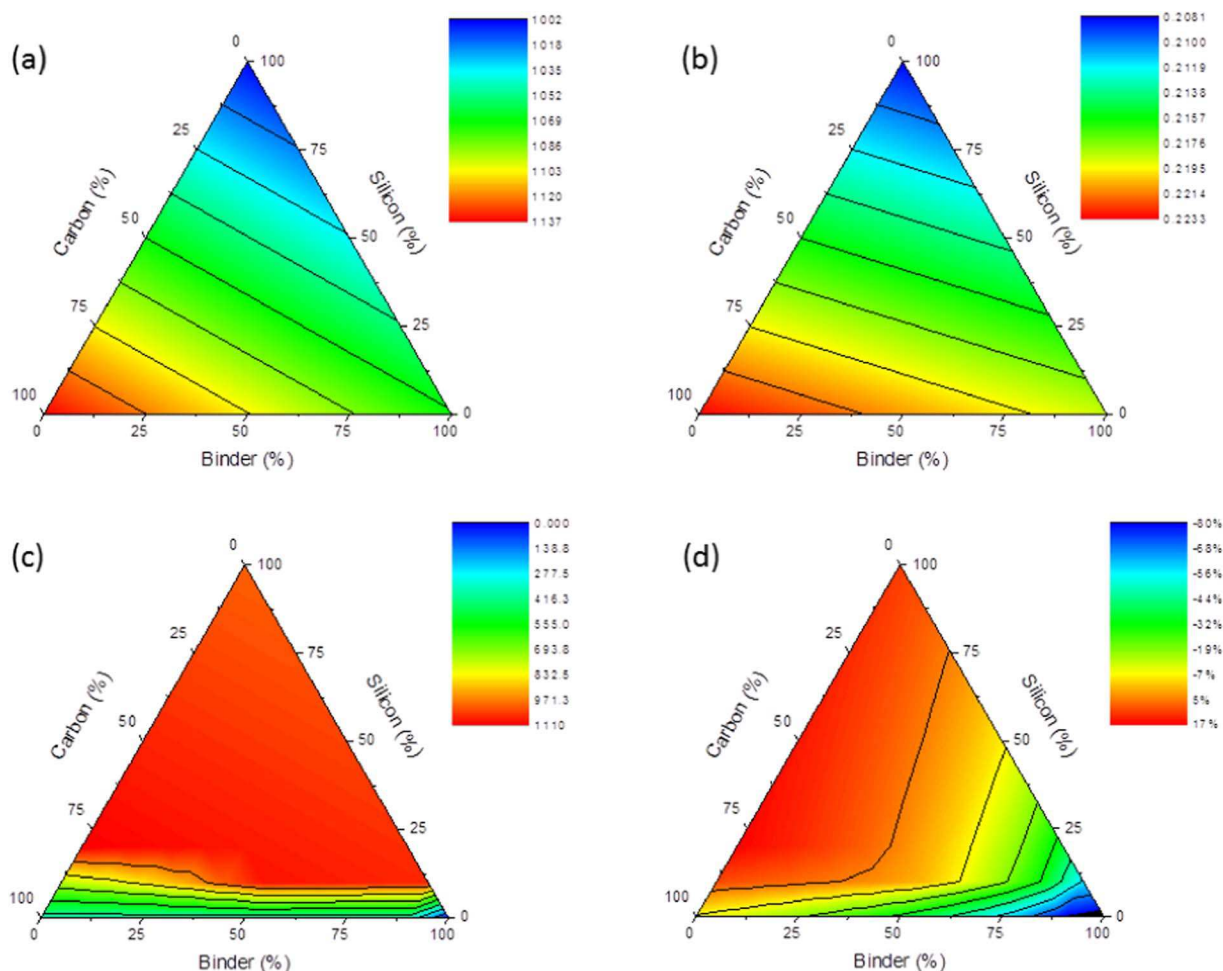
The variables were factored into numerical values and the results were fitted to linear and non-linear models that represent irreversible and reversible capacity. From the results, we have selected the best performing variables, and the fitted models are simplified to optimize silicon, carbon, and binder composition. The selected variables are also shown in Table V.

Our results have shown some obvious outcomes for selecting better performing variables, and the selected parameters are summarized and explained:

• Type of Silicon: Etched and non-ball-milled silicon performed better than other types of silicon. It is well known that the etching of

Table V. Summary of the variables used in the DOE optimization of silicon:carbon:binder anode. Selected variables were obtained from the battery data of 40 different composites. Some of them are shown in Figure 7.

Variables			Selected variables
Silicon	Amount	0∼100 wt%	0∼100 wt%
	Type	Etched or non-etched	Etched
	Process	Ball milled or non-ball milled	Non-ball milled
Carbon	Amount	0∼100 wt%	0∼100 wt%
	Type	CSP, MCMB, G15	MCMB
Binder	Amount	0∼30 wt%	0∼30 wt%
	Type	PTP, PEDOT, NaCMC, NaAlg, PVDF	PTP
Electrolytes	LiPF$_6$ (M)	1 or 1.2	DEC
	Type	DEC, DMC	1 M
Blade	Size (um)	100, 150, 250, 350	100

Figure 8. Calculated (a) reversible and (b) irreversible capacity of the silicon:graphite composite, (c) reversible capacity and (d) percent improvements in full-cell battery.

silicon removes the silicon oxide layers formed during synthesis and handling.[39] Due to its nanometer size, the silicon has a high surface area that allows for the formation of a significant amount of silicon oxide layers that reduces the reversible capacity. Even though it was shown that nano-sized silica is electrochemically active,[40] the results show that the silicon oxide layer at the surface does not provide any benefits to the capacity, but helps in interacting with the binder and other electrode components.[41,42] Our previous results show that ball milling leads to amorphization of crystalline silicon; however, in silicon nanoparticle the amorphization did not improve reversible capacity. The nano-sized silicon might be small enough that amorphization is not required.[30]

- Type of Graphitic carbon: Mesoporous carbon microbeads (MCMB) provided better performance from the experimental results; the main reason is the good and well-known reversibility. It also acts as a buffer to mitigate the volume expansion due to the negligible volume expansion during lithiation.
- Type of electrolyte: 1 M LiPF$_6$ in DEC showed better performance compared to DMC when used with 1 M of LiPF$_6$.
- The thickness of the "Laminate" cast: The thickness had no effect on the performance.

The battery data were fitted to linear and non-linear models to find an estimation of irreversible and reversible capacities. The linear model was selected since the theoretical capacities from the ternary diagram have shown linear relation as shown in Figure 3. However, it is also known experimentally that the capacity of the composite does not show a linear relation due to many factors, such as irreversible

capacity, volume expansion, the size of the particles, type of electrolyte or binder. The results of the linear model, which is shown in Figures 8a and 8b, shows a decrease in irreversible and reversible capacity as the number of silicon increases. Also, some compositions show higher-than-theoretical capacity due to the linear fitting. For non-linear fitting, shown in supporting information Figure S3 b and d, the results show unreasonable values such as negative values for irreversible and reversible capacity or higher-than-theoretical values for capacity. As a result, we have set limits for theoretical capacity, so the capacity does not go below zero or exceeds theoretical capacity and the results are shown in Figure 8c for linear model and for non-linear models are shown in supporting information, Figure S4. Setting up the limits was necessary to use Equation 4 and find the optimized ratio of the composites.

The estimations from Figures 8b and 8c are used along with Equation 4 to calculate improvements on a full-cell battery that is shown in Figure 8d. Figure 9c shows that the maximum experimental reversible capacity from the fitted model is 1100 mAh/g. This is true for most of the ternary diagrams and is way lower than the full theoretical capacity of the silicon (4200 mAh/g). The low capacity of the silicon composites could be improved in the future, however, the results obtained so far do not have enough data point to cover the whole range of parameters, which causes the lower than expected capacity. Some research groups have reported capacities in the range between 1000 to 4000 mAh/g,[14,23,43] but this was in special experimental conditions such as low loading, thin films, low C-rates. Some of the cells tested were assembled with close to the optimum composition of 10:75:15 (Si:Carbon:binder with a theoretical capacity of
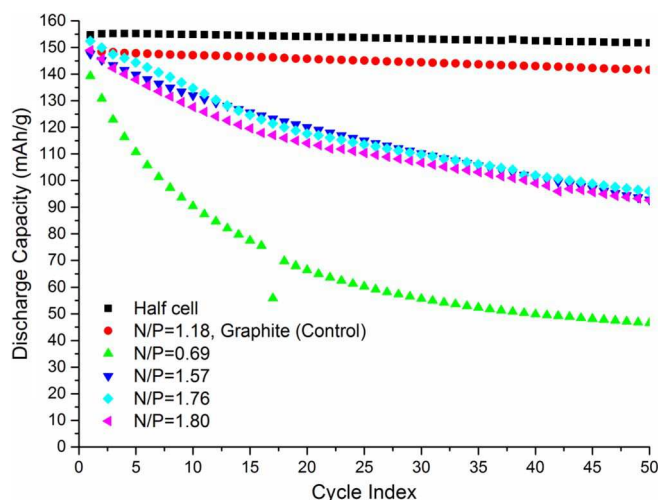
Figure 9. Li-ion full cells using silicon:graphite composite and NMC cathode.

Figure 10. Potential and dQ/dV profile of Graphite/NMC full-cell.

700 mAh/g), which only have shown 465 mAh/g. The battery results of the silicon composite tested in this work still provide a trend that will help in the optimization of the silicon composites. Figure 8d shows that a maximum of 16% improvement can be achieved when the amount of silicon exceeds 10 wt%. However, the capacity yields are way below 25% which suggests the optimum amount of silicon that gives the highest improvement in the total cell capacity/energy density is between 10 and 25 wt% of silicon in a composite. Figure 9b shows the irreversible capacity averages around 20–23%, which is also a non-realistic estimate since using carbon will provide lower than 10% irreversible capacity. This mismatch is also caused by the linear fitted model. Another reason might be due to the type of carbon tested in this work, for example, the carbon super S, which is additive, would provide higher irreversible capacity compared to MCMB that shown around 6% of irreversible capacity. Also, silicon usually has more than 20% of irreversible capacity. By considering the irreversible capacity of each material, the composite that provides around 20% of irreversible capacity is reasonable to use to find the estimation of the improvements in the full cell. Irreversible and reversible capacities from Figures 8b and 8c are used with Equation 4 to generate Figure 8d. More than 5 wt% of silicon has to be used with the minimum amount of binder to obtain improvements in the full-cell; however, more than 25 wt% of silicon is not necessary since the capacity yields are less than 25%.

Performance of silicon/graphite composites in full Li-ion cells.—
To verify the results, we have tested some of the composites in full cells using NMC as a cathode. One of the first challenges faced was to balance the capacity of the active materials in both electrodes: cathode (P) and anode (N) in a coin cell. Full cells with different N/P ratios ranging from 0.7 to 1.9 were assembled. The full-cell and NMC/Li half-cell discharge capacity results are shown in Figure 9. The composition of the anode was 10 wt% silicon, 85 wt% MCMB, and 5 wt% sodium alginate as a binder. The composition of the cathode was 90 wt% NMC, 5 wt% carbon Super P, and 5 wt% PVDF. The electrolyte was 1 M LiPF$_6$ in EC:DEC (3:7) with 10% fluoroethylene carbonate (FEC) as additive. The most optimized discharge capacity was achieved when N/P was at 1.76. However, the optimized full cells still show a continuous decrease in capacity reaching 63% of 95 mAh/g after 50 cycles.

For further analysis, the potential profile and dQ/dV are plotted as shown in Figure 10, Figure 11, and in supporting information. Figure 10 and Figure 11 are for graphite/NMC full-cell and Si composite/NMC full-cell (N/P = 1.76) respectively. Figure 10 shows the full-cell battery of NMC with graphite as an anode. The distinctive peaks at 3.4, 3.5 and 3.7 V when charging and discharging are due to the lithiation and de-lithiation of graphite. The first dQ/dV cycle
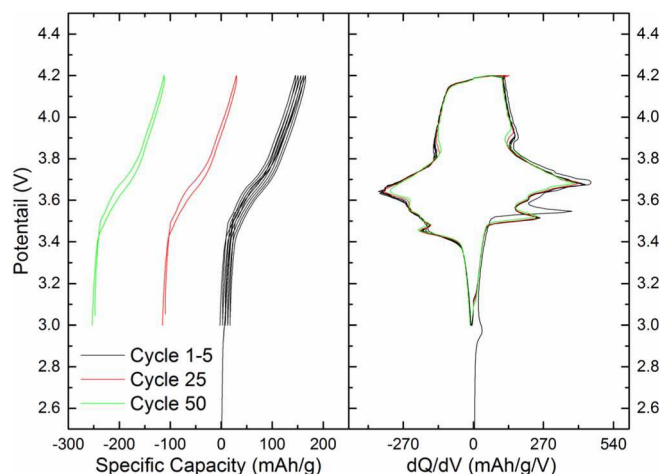
shows a slightly higher shift, 0.5 V higher, due to the SEI formation on graphite at first lithiation, which is due to the slightly higher average potential against Li/Li$^+$. The consistent dQ/dV profile explains the balanced active materials in a cathode and anode. Unlike graphite, Si-composite in full cells exhibits broader peaks because of the lithium alloying reaction, not like graphite where lithium intercalates and results in sharper peaks. Even though the silicon/NMC full cell (N/P = 1.76) has the best capacity retention among the others, the dQ/dV profile show reduced peak current, a shift in potential and even disappearance of some peaks. The shift in potential has also been observed by others and was attributed to the higher end of charging voltages.[44] This effect might be caused by the continuous formation of SEI at silicon surface and a decrease in reversible capacity. We were hoping to improve the reversibility of the silicon composite by balancing the active material of cathode and anode, but obviously, further work is required to optimize the silicon composite anode to work in a full-cell, Li-ion battery as it was pointed out by other researchers.[44–46]

Moreover, due to the challenges faced with this new type of full cells, it was hard to move to compositions with higher silicon content than 10 wt% until the issues with capacity fade are resolved. This, of course, requires the discovery of new electrolyte additives, binders and other components in the battery.
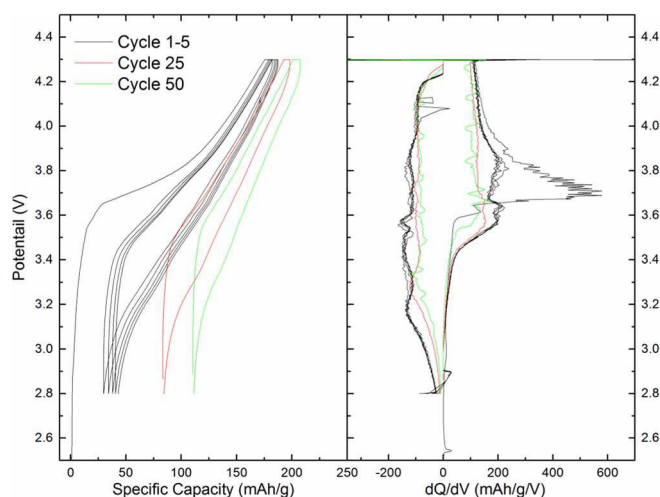

Figure 11. Potential and dQ/dV profile of silicon:graphite composite/NMC full-cell with 1.76 of N/P.

Conclusions

In this work, we have evaluated the performance of silicon-graphitic carbon composites in half and full Li-ion cells. We first optimized silicon:graphite composites using a newly modified equation based on the work of Obrovac et al.[29] From calculations, we found that 59% improvement in energy density can be obtained when only 6% irreversible capacity is assumed. However, using half cells experimental results, lower improvements are achieved in graphite-rich composites with low silicon content reaching 16% improvements when 20% of silicon and 80% of graphite is used with no binder, which was due to the high irreversible and low reversible capacity. Realistically, the range of the silicon would be from 15 to 25% of silicon, 50% to 80% of graphite and 5 to 10% of binder. The calculated improvements in this work were based on gravimetric capacity, but similar results have been obtained when theoretical limits were estimated using volumetric capacity and using simple mass balance equations.[38] We found that assembling full cells using the silicon:graphite composite is not straightforward and requires lots of optimization to improve coulombic efficiency and cycleability. For examples, full cells assembled with 10 wt% silicon:graphite composite give 63% capacity retention of 95 mAh/g after only 50 cycles.

Acknowledgment

References

1. G.-A. Nazri and G. Pistoia, *Lithium Batteries: Science and Technology*, Kluwer Academic Publisher, Boston, Dordrecht, New York, London (2003).
2. A. D. W. Todd, P. P. Ferguson, M. D. Fleischauer, and J. R. Dahn, *International Journal of Energy Research*, **34**(6), 535 (2010).
3. M. Yoshio, T. Tsumura, and N. Dimov, *J. Power Sources*, **146**(1-2), 10 (2005).
4. J. Li, D.-B. Le, P. P. Ferguson, and J. R. Dahn, *Electrochim. Acta*, **55**(8), 2991 (2010).
5. H. Groult, H. El Ghallali, A. Barhoun, E. Briot, C. M. Julien, F. Lantelme, and S. Borensztjan, *Electrochim. Acta*, **56**(6), 2656 (2011).
6. P. Poizot, S. Laruelle, S. Grugeon, L. Dupont, and J. M. Tarascon, *Nature*, **407**(6803), 496 (2000).
7. F. M. Courtel, Y. Abu-Lebdeh, and I. J. Davidson, *Electrochim. Acta*, **71**, 123 (2012).
8. C. K. Chan, H. Peng, G. Liu, K. McIlwrath, X. F. Zhang, R. A. Huggins, and Y. Cui, *Nat. Nanotechnol.*, **3**(1), 31 (2008).
9. D. Larcher, S. Beattie, M. Morcrette, K. Edstrom, J. C. Jumas, and J. M. Tarascon, *J. Mater. Chem.*, **17**(36), 3759 (2007).
10. J. Li, R. B. Lewis, and J. R. Dahn, *Electrochem. Solid-State Lett.*, **10**(2), A17 (2007).
11. U. Kasavajjula, C. Wang, and A. J. Appleby, *J. Power Sources*, **163**(2), 1003 (2007).
12. D. GOLODNITSKY and E. PELED, in *Lithium-Ion Batteries*, p. 1, (2004).
13. Y. Yang, M. T. McDowell, A. Jackson, J. J. Cha, S. S. Hong, and Y. Cui, *Nano Lett.*, **10**(4), 1486 (2010).
14. A. Magasinski, B. Zdyrko, I. Kovalenko, B. Hertzberg, R. Burtovyy, C. F. Huebner, T. F. Fuller, I. Luzinov, and G. Yushin, *ACS Appl. Mater. Interfaces*, **2**(11), 3004 (2010).
15. J. B. Chen, H. L. Zhao, J. C. He, and J. Wang, *Rare Metals*, **30**(2), 166 (2011).
16. M. S. Park, Y. M. Kang, S. Rajendran, H. S. Kwon, and J. Y. Lee, *Mater. Chem. Phys.*, **100**(2-3), 496 (2006).
17. G. X. Wang, L. Sun, D. H. Bradhurst, S. Zhong, S. X. Dou, and H. K. Liu, *J. Alloys Compd.*, **306**(1-2), 249 (2000).
18. M. N. Obrovac and L. J. Krause, *J. Electrochem. Soc.*, **154**(2), A103 (2007).
19. S. Komaba, N. Yabuuchi, T. Ozeki, K. Okushi, H. Yui, K. Konno, Y. Katayama, and T. Miura, *J. Power Sources*, **195**(18), 6069 (2010).
20. Y. Kobayashi, S. Seki, Y. Mita, Y. Ohno, H. Miyashiro, P. Charest, A. Guerfi, and K. Zaghib, *J. Power Sources*, **185**(1), 542 (2008).
21. J. S. Bridel, T. Azais, M. Morcrette, J. M. Tarascon, and D. Larcher, *Chem. Mater.*, **22**(3), 1229 (2010).
22. S. Komaba, K. Shimomura, N. Yabuuchi, T. Ozeki, H. Yui, and K. Konno, *The Journal of Physical Chemistry C*, **115**(27), 13487 (2011).
23. I. Kovalenko, B. Zdyrko, A. Magasinski, B. Hertzberg, Z. Milicev, R. Burtovyy, I. Luzinov, and G. Yushin, *Science*, **334**, 75 (2011).
24. N.-S. Choi, K. H. Yew, W.-U. Choi, and S.-S. Kim, *J. Power Sources*, **177**(2), 590 (2008).
25. N. Yabuuchi, K. Shimomura, Y. Shimbe, T. Ozeki, J.-Y. Son, H. Oji, Y. Katayama, T. Miura, and S. Komaba, *Advanced Energy Materials*, **1**(5), 759 (2011).
26. A. Guerfi, P. Charest, M. Dontigny, J. Trottier, M. Lagacé, P. Hovington, A. Vijh, and K. Zaghib, *J. Power Sources*, **196**(13), 5667 (2011).
27. N. Salem, M. Lavrisa, and Y. Abu-Lebdeh, *Energy Technology*, **4**(2), 331 (2015).
28. G. Liu, S. Xun, N. Vukmirovic, X. Song, P. Olalde-Velasco, H. Zheng, V. S. Battaglia, L. Wang, and W. Yang, *Adv. Mater. (Weinheim, Ger.)*, **23**(40), 4679 (2011).
29. M. N. Obrovac and V. L. Chevrier, *Chem. Rev. (Washington, DC, U. S.)*, **114**(23), 11444 (2014).
30. C.-H. Yim, F. M. Courtel, and Y. Abu-Lebdeh, *Journal of Materials Chemistry A*, **1**(28), 8234 (2013).
31. M. N. Obrovac, L. Christensen, D. B. Le, and J. R. Dahn, *J. Electrochem. Soc.*, **154**(9), A849 (2007).
32. L. F. Nazar and O. Crosnier, in "*Lithium Batteries*", p. 112, 2003.
33. J. H. Lee, H. M. Lee, and S. Ahn, *J. Power Sources*, **119–121**, 833 (2003).
34. K.-Y. Oh, J. B. Siegel, L. Secondo, S. U. Kim, N. A. Samad, J. Qin, D. Anderson, K. Garikipati, A. Knobloch, B. I. Epureanu, C. W. Monroe, and A. Stefanopoulou, *J. Power Sources*, **267**, 197 (2014).
35. S.-i. Tobishima, K. Takei, Y. Sakurai, and J.-i. Yamaki, *J. Power Sources*, **90**(2), 188 (2000).
36. M. E. Spahr, in *Lithium-Ion Batteries: Science and Technologies*, p. 117, (2009).
37. F. Luo, B. Liu, J. Zheng, G. Chu, K. Zhong, H. Li, X. Huang, and L. Chen, *J. Electrochem. Soc.*, **162**(14), A2509 (2015).
38. R. Dash and S. Pannala, *Scientific Reports*, **6**, 27449 (2016).
39. S. Xun, X. Song, L. Wang, M. E. Grass, Z. Liu, V. S. Battaglia, and G. Liu, *J. Electrochem. Soc.*, **158**(12), A1260 (2011).
40. B. Guo, J. Shu, Z. Wang, H. Yang, L. Shi, Y. Liu, and L. Chen, *Electrochem. Commun.*, **10**(12), 1876 (2008).
41. B. Koo, H. Kim, Y. Cho, K. T. Lee, N.-S. Choi, and J. Cho, *Angewandte Chemie International Edition*, **51**(35), 8762 (2012).
42. H. Wu, G. Yu, L. Pan, N. Liu, M. T. McDowell, Z. Bao, and Y. Cui, *Nature Communications*, **4**, 1943 (2013).
43. A. Magasinski, P. Dixon, B. Hertzberg, A. Kvit, J. Ayala, and G. Yushin, *Nat. Mater.*, **9**(4), 353 (2010).
44. S. D. Beattie, M. J. Loveridge, M. J. Lain, S. Ferrari, B. J. Polzin, R. Bhagat, and R. Dashwood, *J. Power Sources*, **302**, 426 (2016).
45. M. Klett, J. A. Gilbert, K. Z. Pupek, S. E. Trask, and D. P. Abraham, *J. Electrochem. Soc.*, **164**(1), A6095 (2017).
46. N. Delpuech, N. Dupre, P. Moreau, J.-S. Bridel, J. Gaubicher, B. Lestriez, and D. Guyomard, *ChemSusChem*, **9**(8), 841 (2016).